UNIFIED SKYRME APPROACH TO THE REAL AND IMAGINARY PARTS OF THE HEAVY ION OPTICAL POTENTIAL

R. SARTOR and Fl. STANCU

Institut de Physique B5, Université de Liège, Sart Tilman,

B-4000 LIEGE 1, Belgium.

ABSTRACT : We derive a set of energy dependent Skyrme interaction parameters to be used in the calculation of the complex heavy ion optical potential. They are determined by fitting the binding energy of ^{16}O as well as nuclear matter constants and the real volume part of the $^{16}O + ^{16}O$ optical potential previsously obtained from the Reid soft core interaction. For the binding energy of heavier nuclei and the single particle levels the present parameters lead to predictions comparable with those of other Skyrme interactions.

1. INTRODUCTION

A current procedure [1-4]) is to define the heavy ion optical potential for a separation distance D between nuclei as

$$V_{opt}(D) = \langle \psi(D) | H | \psi(D) \rangle - \langle \psi(\infty) | H | \psi(\infty) \rangle \qquad (1.1)$$

i.e. as the difference between the expectation values at distance D and at infinity of an effective hamiltonian

$$H = \sum_i t_i + \frac{1}{2} \sum_{i \neq j} v_{ij} \quad . \qquad (1.2)$$

In ref. [3]) use was made of the Skyrme interaction energy density obtained in [5]). Accordingly, only the real part of the optical potential has been calculated. On the other hand, in Ref. [4]) the effective interaction v_{ij} was complex since it was defined as an average [6]) over the non-hermitian G-matrix associated with a deformed Fermi sea [7-11]). Hence eq. (1.1) yielded both the real and imaginary parts of the heavy ion optical potential.

As the method of Ref. [3]) is appealing both for physical and computational reasons, we proposed in Refs. [12]) and [13]) a complex energy density formalism for the calculation of the heavy ion potential. In Ref. [12]) the imaginary part of the energy density was introduced through a scaling factor which is a function of the local matter and kinetic energy densities. In ref. [13]), this goal was achieved by extending the density matrix expansion [14]) to the complex domain. Both

approaches nicely reproduced the imaginary part of the $^{16}O + ^{16}O$ optical potential calculated in Ref. [4]) from the above-mentioned complex finite range interaction. However some discrepancies remained for the real part of V_{opt} . In Ref. [12]) we have used the set SIII of the Skyrme interaction parameters obtained in [15]) for entirely different purposes. Hence a discrepancy with respect to the exact calculation was natural. For the density matrix approach we refer to the discussion given in Ref. [13]).

In this work we want to find a complex Skyrme interaction which leads to a unified derivation of both the real and imaginary parts of the "exact" $^{16}O + ^{16}O$ optical potential [4]). This is explained in section 2 where our fitting procedure is described in detail. It will turn out that we have to allow for an energy dependence of the Skyrme interaction parameters as discussed in section 3. In section 4, we show the predictions of the present Skyrme interaction sets for the imaginary part of the $^{16}O + ^{16}O$ optical potential.

2. THE SKYRME APPROACH AND THE REAL PART OF THE HEAVY ION OPTICAL POTENTIAL

In the present section by applying a fitting procedure we derive a set of Skyrme interaction parameters t_o, t_1, t_2, t_3, W_o, x_o which reproduce well the real part of the $^{16}O + ^{16}O$ potential calculated in [4]). Besides the $^{16}O + ^{16}O$ potential we also want to reproduce the Reid soft core nuclear matter potential energies for a series of configurations of two

Fermi spheres separated by the distance K_r between their centres. Each of these configurations given in Table 1 is labelled by its density ρ and intrinsic kinetic energy $\tau^{(2)}$ [10,12])

$$\tau^{(2)} = \tau - \frac{j^2}{\rho} \tag{2.1}$$

where τ is the kinetic energy density and j is the current density. For $K_r = 0$, i.e. a single sphere, we impose constraints on the fit such as to obtain good agreement between the calculated Skyrme-Hartree-Fock (SHF) binding energy of ^{16}O and experimental value. The Skyrme parameters obtained by a least square fit are gathered together in Table 2. The values of t_i (i = 0,1,2,3) for $K_r = 0$ give $k_F = 1.36\ fm^{-1}$, $E/A = -16.6$ MeV, $K = k_F^2 \frac{\partial^2 E/A}{\partial k_F^2} = 346$ MeV, $m^*/m = 0.51$ for the nuclear matter.

We now indicate the main steps of our procedure and discuss the quality of the fit.

The Skyrme interaction energy density used in our calculations has the form [5]) :

$$\begin{aligned} H = {} & \frac{\hbar^2}{2m}\tau + \frac{1}{2}t_o\left[(1+\frac{1}{2}x_o)\rho^2 - (x_o+\frac{1}{2})(\rho_n^2+\rho_p^2)\right] + \\ & + \frac{1}{4}(t_1+t_2)\rho\tau + \frac{1}{8}(t_2-t_1)(\rho_n\tau_n+\rho_p\tau_p) + \\ & + \frac{1}{16}(t_2-3t_1)\rho\nabla^2\rho + \frac{1}{32}(3t_1+t_2)(\rho_n\nabla^2\rho_n+\rho_p\nabla^2\rho_p) \\ & + \frac{t_3}{4}\rho_n\rho_p\rho - \frac{1}{2}W_o(\rho\,\underset{\sim}{\nabla}\cdot\underset{\sim}{J} + \rho_n\,\underset{\sim}{\nabla}\cdot\underset{\sim}{J}_n + \rho_p\,\underset{\sim}{\nabla}\cdot\underset{\sim}{J}_p) \\ & + H_c \end{aligned} \tag{2.2}$$

where ρ_n (ρ_p) are the nucleon densities, τ_n (τ_p) the kinetic energy densities and $\underset{\sim}{J}_n$ ($\underset{\sim}{J}_p$) the spin densities. The exchange contribution of the Coulomb part H_c is treated as in Ref.[15]).

For N = Z nuclei one can see that this expression has several distinct contributions [5]) : a kinetic energy and a Coulomb term both free of parameters, a volume contribution depending on t_o, t_3 and the combination $\frac{1}{16}$ $(3t_1 + 5\ t_2)$, a surface term related to the density gradient and proportional to $\frac{1}{64}$ $(9t_1 - 5t_2)$ and a spin-orbit term with the strength W_o . The SHF binding energy of ^{16}O appeared to be sensitive to the value taken by the surface term. The best combined fit of V_{opt} at $K_r = 0$ and of the ^{16}O binding energy was obtained with $\frac{1}{64}$ $(9t_1 - 5t_2) = 90$ MeV fm^{-5} . The spin orbit coupling has a minor contribution of the order of 1 MeV to the total binding energy of ^{16}O. Values in the range W_o = 100-120 MeV fm^5 closely reproduce the splitting of the neutron and proton 1p-levels in ^{16}O. But for heavier nuclei the spin-orbit part has a larger contribution to the total binding energy. We choose W_o = 120 MeV fm^5 which overbinds ^{40}Ca and ^{56}Ni by less than 1%. The parameter x_o affects the binding energy of $N \neq Z$ nuclei only. The range $x_o = 0 - 0.15$ gives for the symmetry energy values between 27.17 MeV and 34.31 MeV. The total binding energy decreases with W_o and increases with x_o . Then the upper limit $x_o = 0.15$ matches favourably with the value chosen for W_o reproducing the binding energies of ^{48}Ca, ^{90}Zr and ^{208}Pb also within less than 1%. The results for the binding energies and the r.m.s charge radii are given in Table 3.

In fig. 1, we compare the SHF level spectra for ^{16}O, ^{40}Ca, ^{48}Ca and ^{208}Pb with experiment. The density of states is qualitatively comparable with that obtained with other Skyrme sets and consistent with the value found for m^*/m which leads to a too small density of states near the Fermi surface. Actually the only serious discrepancy with experiment appears for the nuclear r.m.s charge radii r_c which are underestimated with the present $K_r = 0$ set (see Table 3).

In order to ensure continuity on the parameters t_i considered as a function of K_r, we have imposed the constraint $\frac{1}{64}$ $(9t_1 - 5t_2) = 90$ MeV fm^{-5} also in fitting the real part of V_{opt} at $K_r = 0.5$ and 1 fm^{-1} . In Fig. 2, we display the corresponding fits to the real part of the $^{16}O + {}^{16}O$ optical potential at all three values of K_r. These results, as well as those for the imaginary part are obtained with ρ , τ and j corresponding to fully anti-symmetrized wave functionsof a two center harmonic oscillator shell model. The size parameter is b = 1.8 fm. A detailed discussion of the model is given in Ref. [2]).

3. THE ENERGY DEPENDENCE

The present approach contains two sources of the energy dependence of the optical potential : 1) the dependence of the matter density ρ and especially the kinetic energy densities τ and $\tau^{(2)}$ on the relative momentum K_r, the influence of which was studied in connection with the anti-

symmetrization effect [2,3,16]) and the effective mass [3,16]) ; 2) the explicit dependence of the Skyrme interaction parameters on the bombarding energy. This is the effect of the Pauli principle directly on the effective interaction and was obtained from calculating the G-matrix in a deformed Fermi sea [6,10]). From Table 1 one can notice that t_i (i=0,1,2,3) vary almost linearly with K_r . In order to see the importance of the latter energy dependence, we have calculated V_{opt} by using the parameters t_i for $K_r = 0$ also at $K_r = 0.5$ and 1 fm^{-1}. The results are shown in Fig. 3. The dashed curves therefore contain only the energy dependence given by 1). An important discrepancy with respect to the exact results (full curves) can be noticed for $K_r = 0.5$ fm^{-1} in the tail region and for $K_r = 1$ fm^{-1} at all distances.

4. THE SKYRME APPROACH FOR THE IMAGINARY PART OF THE HEAVY ION OPTICAL POTENTIAL

The analysis of the effective interaction $v_{eff}(r)$ obtained in [6]) from the Reid soft core matrix elements allowed us to introduce in [12]) a ratio ξ between the imaginary and the real part of v_{eff} as a constant with respect to the interacting distance r but depending on the local density ρ and the intrinsic kinetic energy density $\tau^{(2)}$. The approximation made by defining ξ in this way was tested in Ref. [12]) and found to be very good.

Let us call $v_{SK}(r)$ the Skyrme interaction depending on the parameter sets of Table 2. We can define a complex

effective interaction [12])

$$v^c(r) = [1 + i\ \xi(\rho,\tau^{(2)})]\ v_{SK}(r) \quad . \tag{4.1}$$

Such an interaction gives a complex energy density which can be used to consistently calculate both the real and imaginary parts of the optical potential. Its potential part has the form

$$H^{(c)}_{pot} = [1 + i\ \xi(\rho,\tau^{(2)}]\ H_{pot} \tag{4.2}$$

where H_{pot} is the energy density (2.2) without Coulomb, kinetic and spin-orbit terms. Also τ has been replaced by $\tau^{(2)}$ of eq. (2.1) in order to include the relative motion [3]). The results for Im V_{opt} obtained from eq. (4.2) are compared in fig. 4 with those of the exact calculation of ref. [4]). They remain very similar to those of ref. [12]). This reflects the fact that the imaginary part of the optical potential is strongly dominated by the kinetic energy density effects contained in the scaling factor $\xi(\rho,\tau^{(2)})$ and hence does not allow to distinguish between different parameter sets of the Skyrme energy density.

The present interactions can be used in the calculation of V_{opt} for other pairs of nuclei once one has chosen a model to describe the matter and the kinetic energy densities. They can also be used in the study of the energy dependence of the optical potential.

One of us (R.S.) thanks the I.I.S.N. for financial support. We are grateful to D. Vautherin for providing us his Hartree-Fock code.

REFERENCES

1) G. Reidemeister, Nucl. Phys. A197 (1972) 631

2) T. Fliessbach, Z. Phys. 247 (1971) 117

3) D.M. Brink and Fl. Stancu, Nucl. Phys. A243 (1975) 175

4) R. Sartor, A. Faessler, S.B. Khadkikar and S. Krewald, Nucl. Phys. A359 (1981) 467

5) D. Vautherin and D.M. Brink, Phys. Rev. C5 (1972) 626

6) A. Faessler, T. Izumoto, S. Krewald and R. Sartor, Nucl. Phys. A359 (1981) 509

7) D.A. Saloner and C. Toepffer, Nucl. Phys. A283 (1977) 108

8) G.F. Bertsch, Phys. Rev. C5 (1977) 713

9) F. Beck, K.H. Müller and H.S. Köhler, Phys. Rev. Lett. 40 (1978) 837

10) T. Izumoto, S. Krewald and A. Faessler, Nucl. Phys. A341 (1980) 319

11) K.H. Müller, Z. Phys. A295 (1980) 79

12) R. Sartor and Fl. Stancu, Phys. Rev. C24 (1981) 2347

13) R. Sartor and Fl. Stancu, Phys. Rev. C26 (1982) 1025

14) J.W. Negele and D. Vautherin, Phys. Rev. C5 (1972) 1472

15) M. Beiner, H. Flocard, Nguyen Van Giai and P. Quentin, Nucl. Phys. A238 (1975) 29

16) S.A. Moszkowski, Nucl. Phys. A309 (1978) 273.

17) A. Bohr and B. Mottelson, Nuclear Structure (Benjamin, New York, 1969) vol. 1.

TABLE CAPTIONS

Table 1. Reid soft core (RSC, fourth column) nuclear matter potential energies for spherical (K_r = 0 fm^{-1}) and deformed Fermi seas (K_r = 0.5 and 1.0 fm^{-1}) together with their Skyrme fit (fifth column). $\tau^{(2)}$ is defined in the text.

Table 2. Skyrme parameter sets for different values of the relative momentum per nucleon K_r .

Table 3. Experimental and SHF binding energies B and r.m.s charge radii r_c with the Skyrme interaction parameters of Table 2 (K_r = 0). The experimental data are the same as those in Ref. [15]).

FIGURE CAPTIONS

Fig. 1. Experimental and SHF single particle energies e with the Skyrme interaction parameters of Table 2 ($K_r = 0$). The experimental values are from Ref. [17]).

Fig. 2. The real part of the $^{16}O + ^{16}O$ optical potential. The full curves are the Reid soft core results of Ref. [4]), the dashed ones are the present calculations with the Skyrme parameter sets of Table 2. The labels 1,2,3 correspond to $K_r = 0$, 0.5 and 1. fm^{-1}, respectively.

Fig. 3. The real part of the $^{16}O + ^{16}O$ optical potential at two different relative momenta : (a) $K_r = 0.5$ fm^{-1} and (b) $K_r = 1$ fm^{-1}. The full curves are the results of Ref. [4]) and the dashed curves are the present results with Skyrme parameters t_i of Table 2 at $K_r = 0$. The energy dependence is contained only in ρ , τ and $\tau^{(2)}$.

Fig. 4. Imaginary part of the $^{16}O + ^{16}O$ optical potential. The full curves correspond to the results of Ref. [4]) ; the dots are the present calculations with the Skyrme parameter sets of Table 2 and the scaling factor $\xi(\rho,\tau^{(2)})$ of Ref. [12]). The labels 1,2,3 correspond to $K_r = 0$, 0.5 and 1 fm^{-1}, respectively.

TABLE 1

K_r (fm^{-1})	ρ (fm^{-3})	$\tau^{(2)}$ (fm^5)	RSC (MeV/fm^3)	SKYRME (MeV/fm^3)
0.	0.084956	0.059393	- 2.2317	- 2.2355
	0.16991	0.18856	- 6.5150	- 6.7359
	0.25487	0.37063	-11.448	-10.705
0.5	0.084956	0.06055	- 2.2358	- 2.2345
	0.084956	0.06108	- 2.2367	- 2.2309
	0.16991	0.19109	- 6.5095	- 6.7340
	0.25487	0.37462	-11.437	-10.543
1.0	0.084956	0.06323	- 2.2358	- 2.2202
	0.084956	0.06655	- 2.2315	- 2.2109
	0.084956	0.06816	- 2.2241	- 2.2064
	0.16991	0.19640	- 6.4922	- 6.7217
	0.16991	0.20062	- 6.4561	- 6.6981
	0.16991	0.20444	- 6.4229	- 6.6769
	0.25487	0.38285	-11.392	-10.406
	0.25487	0.39132	-11.319	-10.335

TABLE 2

K_r (fm^{-1})	t_o (MeV.fm^3)	t_1 (MeV.fm^5)	t_2 (MeV.fm^5)	t_3 (MeV.fm^6)	x_o	W_o (MeV.fm^5)
0	- 1121.4	638.88	- 2.0190	5174.9	0.15	120
0.5	- 1093.9	587.56	-94.388	8118.7		
1.0	- 1048.8	523.72	-209.30	11541.		

TABLE 3

Nucleus	B^{exp} (MeV)	B^{calc} (MeV)	r_c^{exp} (fm)	r_c^{calc} (fm)
^{16}O	- 127.62	- 127.81	2.73	2.67
^{40}Ca	- 342.06	- 345.00	3.49	3.37
^{48}Ca	- 416.01	- 419.22	3.48	3.41
^{56}Ni	- 484.01	- 481.30	3.75	3.66
^{90}Zr	- 783.92	- 791.16	4.27	4.15
^{208}Pb	- 1636.49	- 1653.90	5.50	5.32

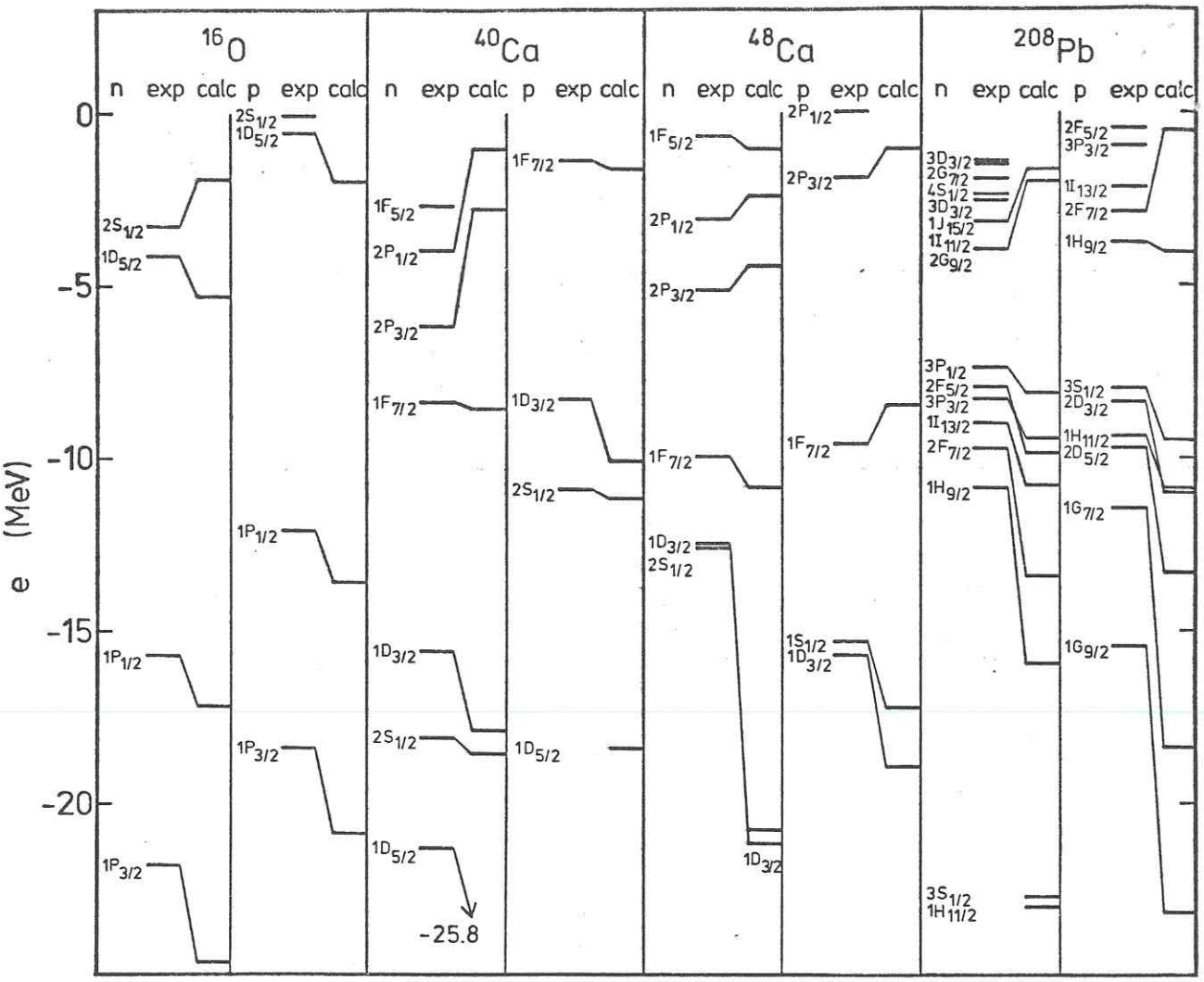
^{16}O
^{40}Ca
^{48}Ca
^{208}Pb
n exp calc p exp calc
e (MeV)
0
-5
-10
-15
-20
$2S_{1/2}$
$1D_{5/2}$
$1P_{1/2}$
$1P_{3/2}$
$1F_{5/2}$
$2P_{1/2}$
$2P_{3/2}$
$1F_{7/2}$
$1D_{3/2}$
$2S_{1/2}$
$1D_{5/2}$
-25.8
$1F_{5/2}$
$2P_{1/2}$
$2P_{3/2}$
$1F_{7/2}$
$1D_{3/2}$
$2S_{1/2}$
$1D_{3/2}$
$2P_{1/2}$
$2P_{3/2}$
$1F_{7/2}$
$1S_{1/2}$
$1D_{3/2}$
$3D_{3/2}$
$2G_{7/2}$
$4S_{1/2}$
$3D_{3/2}$
$1J_{15/2}$
$1I_{11/2}$
$2G_{9/2}$
$3P_{1/2}$
$2F_{5/2}$
$3P_{3/2}$
$1I_{13/2}$
$2F_{7/2}$
$1H_{9/2}$
$3S_{1/2}$
$1H_{11/2}$
$2F_{5/2}$
$3P_{3/2}$
$1I_{13/2}$
$2F_{7/2}$
$1H_{9/2}$
$3S_{1/2}$
$2D_{3/2}$
$1H_{11/2}$
$2D_{5/2}$
$1G_{7/2}$
$1G_{9/2}$

Fig. 1

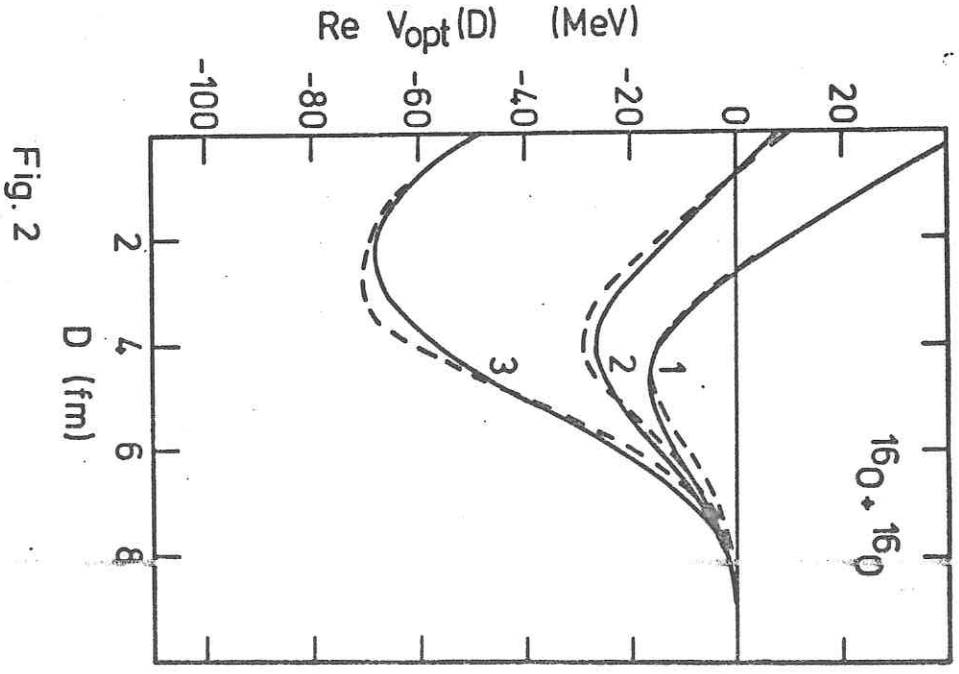
Re V_{opt}(D) (MeV)
-100
-80
-60
-40
-20
0
20
D (fm)
2
4
6
8
1
2
3
$^{16}O + ^{16}O$

Fig. 2

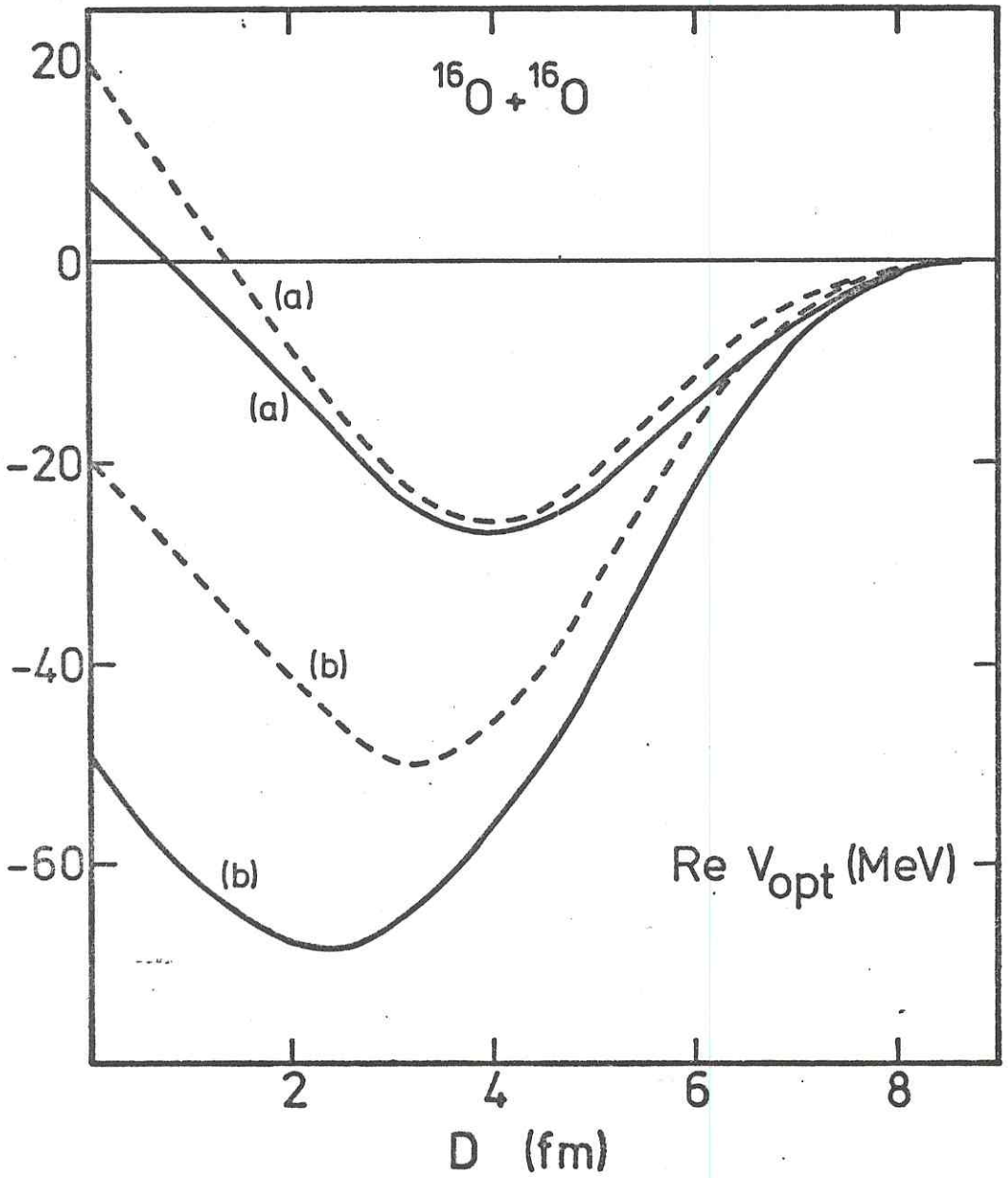
$^{16}O + ^{16}O$
20
0
-20
-40
-60
(a)
(a)
(b)
(b)
Re V_{opt} (MeV)
2
4
6
8
D (fm)

Fig. 3

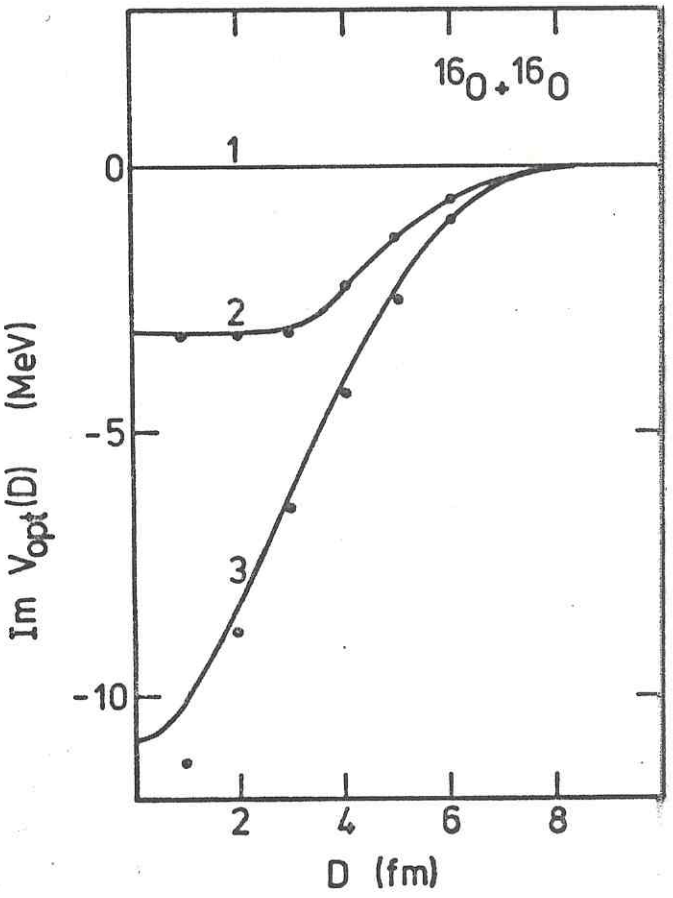
$^{16}O + ^{16}O$
1
2
3
0
-5
-10
Im V_{opt}(D) (MeV)
2
4
6
8
D (fm)

Fig. 4